Chapter 8
Facile Fabrication of 1-D Hierarchical TiO_2 Nanomorphology and Its Application in Dye Sensitized Solar Cell

Asha Anish Madhavan

Abstract One-dimensional nanofibers fabricated by the process of electrospinning have found engaging applications in the field of dye sensitized solar cells (DSSC) due to semi-directed electron transport. Current research accounts for the development of conductive mats made from nanofibers, which is achieved through the electrospinning of TiO_2–ZnO composites and by using polyvinylpyrrolidine as a carrier solution. This fiber was annealed at 450 °C to attain a continuous network of conducting nanofibers. ZnO from the composite was selectively etched to fabricate high surface area anisotropic TiO_2 hierarchical fiber. Morphological and phase analysis conducted by scanning electron microscopy and X-ray diffraction studies confirmed the formation of anatase phase and 1-D hierarchical morphology of TiO_2. These structures were employed as photoanodes in DSSC, which had shown superior photoconversion efficiency.

Keywords TiO_2 · ZnO · Electrospinning · Hydrothermal · Photoanode · DSSC

8.1 Introduction

A wide variety of wide band gap semiconductor oxides like TiO_2, ZnO, SnO_2 and Nb_2O are used for the fabrication of working electrodes which is used in DSSC [1]. The most commonly used metal oxide is TiO_2 because of its versatile properties like thermal and chemical stability, inertness to the electrolyte, non-toxicity, cheap, abundance and many more. Light absorption and light scattering are considered as the main function of TiO_2 electrode. Also, photoanode plays a major role in charge transport and reduction in charge recombination. Based on the modification in the architectures, alteration in morphology, particle size, pore size and distribution and thickness of the thin film, maximum light harvesting can be obtained. In spite of the prospective advantages of DSSC, the net efficiencies are still lacking as compared to the conventional cells. One of the major drawbacks is the insufficient light harvesting

A. A. Madhavan (✉)
Amity University Dubai, Dubai International Academic City, Dubai, UAE
e-mail: amadhavan@amityuniversity.ae

V. K. Jain et al. (eds.), *Advances in Solar Power Generation and Energy Harvesting*, Springer Proceedings in Energy,
https://doi.org/10.1007/978-981-15-3635-9_8

caused by the TiO_2 [2–4]. Improved dye loading and better light scattering can also increase the performance of the DSSC. This can be achieved by replacing randomly oriented TiO_2 nanoparticle with highly organized mesoporous TiO_2 structures [5]. Mesoporous TiO_2 has a continuous network which can provide high surface area, better mass diffusion and hence can facilitate the reactions faster with higher reaction sites [6]. The mesoporous structure mainly depends on the fabrication process, and the pore size distribution can be manipulated by controlling the slurry of the TiO_2 [7, 8]. In an electrode charge, traps determine the electron transport and transfer dynamics. The primary disadvantage of the nanoparticle is the extraordinarily small diffusion coefficient. Nanoparticles with disordered arrangement can lead to lattice mismatches at the grain boundaries. It has been proved that a nanoparticulate matrix having a thickness of 10 mm had shown ~10^6 grain boundaries [10]. This will lead to an accumulation of electrons in the quasi-Fermi level, and hence, the recombination. In addition to this, another important parameter is the slow electron transport through the randomly oriented nanoparticle [11]. Many studies had been conducted to address this issue by replacing nanoparticle with one-dimensional morphologies like nanorods, nanowires, nanotubes, etc., in which the electron transport was proven to be in the direct conduction pathway [12–14]. It has also been proved that the interconnecting meso and micro prechannels in the titania film can result in the effective dye absorption, light scattering and effective percolation of the electrolyte [15]. Kislyuk et al., had proved that TiO_2 nanowires had shown almost four times larger dye absorption as compared to P-25 [16] as it act as a single crystal. However, crystalline structure depends on the fabrication process.

Many techniques have been developed to formulate one-dimensional nanostructured semiconductor oxides developed from template-based synthesis [17], template-free productions [18], by self-assembly method [19], electrospinning, [20] etc. Among these methods, electrospinning is a unique technique which offers the advantage of cost effectiveness, simple and can fabricate nanofibers with varied compositions and morphologies. Due to the semi-directed electron transport, one-dimensional nanofibers have been researched and exhibit a wide array of applications in DSSC [21]. Further, the presence of straight pores in these fibers facilitates the intercalation/de-intercalation of ions, [20, 22] etc. In spite of these appealing aspects, the electrospun TiO_2 materials have very low surface areas. It has already been proved that titanate route can be used for increasing the surface area. In this methodology, TiO_2 is chemically transformed into sodium/potassium titanate and then subsequently converted back to TiO_2. This process is a two-step hydrothermal process which is time-consuming [23]. However, simple approaches for getting high surface area along with guided electron transport are lacking in the literature. In the present study, a two-step process of electrospinning of a bicomponent system (TiO_2–ZnO) is followed by the selective etching of one component (ZnO) to fabricate high surface area anisotropic TiO_2 1-D hierarchical fiber. These nano-morphologies were employed as photoanodes, which had shown superior photoconversion efficiency.

8.2 Experimental

8.2.1 Chemicals and Reagents

The chemicals used in this study are acetone and methanol (Nice Chemicals), polyvinylpyrrolidone (PVP), titanium (IV) isopropoxide, glacial acetic acid, lithium iodide, iodine, acetonitrile and tertiary butyl pyridine, acetonitrile and teri-butanol (Sigma Aldrich), ruthenium (II) dye (N719) and butyl methyl imadizolium iodide, (Solaronix). The substrates used in this study were ITO conductive glass cleaned by sonicating with dilute soap solution, distilled water, acetone and then finally with methanol for 15 min each and then dried prior to use.

8.2.2 Fabrication of TiO_2–ZnO Fiber Composite

In the electrospinning process, polyvinylpyrrolidone (PVP) was used as the carrier polymer. Solution for the electrospinning process was prepared by dissolving PVP in a mixture of methanol and acetic acid. The PVP solution along with the addition of titanium isopropoxide and zinc acetate was made to completely dissolve at room temperature under constant stirring conditions. A syringe was then filled with the blend solution which was subsequently fed into an electrospinning setup (Zeonics System, India). The time and temperature for the electrospinning process were 6 h and 28 °C which was undertaken with a flow rate of 0.5 and an externally applied potential of 15 kV with a tip-to-collector space of 10 cm. The relative humidity was maintained constant of ~55%. The process of electrospinning was carried out with Al foils with dimensions 12 cm × 12 cm × 0.2 mm. After the electrospinning process, these samples were peeled off as a mat and annealed at 450 °C for 2 h to sublimate the binder PVP from the electrospun mats.

8.2.3 Fabrication of TiO_2 1-D Hierarchical Fiber

About 300 mg of the TiO_2–ZnO (TZ), composite fibers were added to the acetic acid solution for the selective etching of ZnO. This solution was introduced into a hydrothermal setup consisting of a 100 mL Teflon-lined container followed by heating at 180 °C. After the annealing, the resultant product was filtered and washed thoroughly with deionized water and with methanol. The resultant anisotropic fibers obtained were then dried at 80 °C in an oven. Based on the components and morphology samples are designated as TiO_2–ZnO fiber (TZ) and 1-D hierarchical fiber (TH), respectively. These morphologies were used for the anode fabrication of DSSC (Fig. 8.1).

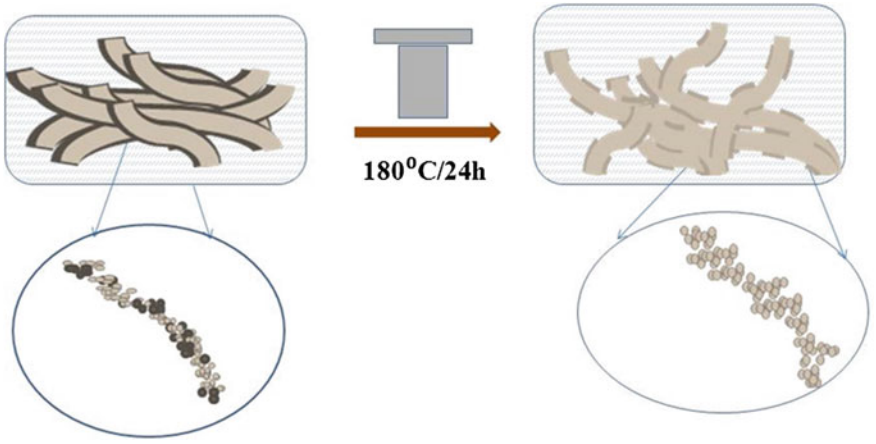

Fig. 8.1 Schematic representation of the synthesis of one-dimensional hierarchical TiO_2 fiber. *Source* Fig 8.1 is reproduced from author PhD thesis. Reference is https://shodhganga.inflibnet.ac.in/bitstream/10603/40981/15/15_synopsis.pdf

8.3 Results and Discussion

8.3.1 Morphological and Phase Analysis

Morphological and phase analysis of nanofibrous mats were analyzed using scanning electron microscopy (SEM) and X-ray diffraction methods. Figure 8.2a and b shows the SEM images of pre-annealed and post-annealed samples of TiO_2–ZnO fiber (TZ), whereas Fig. 8.2c shows the image of TH fibers. It was clearly observed that the TZ fibers were smooth and continuous. The formation of hierarchical structures is induced by the acidic treatment resulting in the selecting etching of ZnO by the in situ dissolution of ZnO as zinc acetate. The smooth surface of the nanofibers got distorted resulting in the formation of pits and humps when TZ is converted to TH

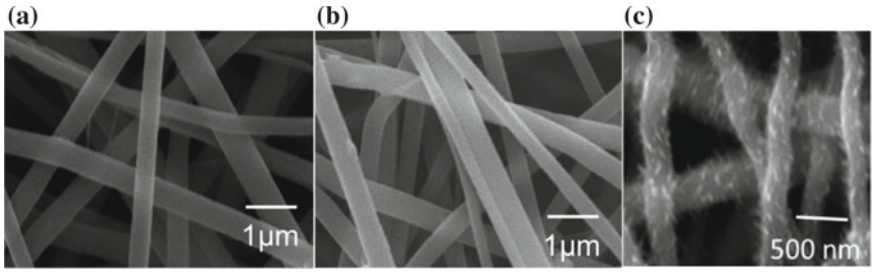

Fig. 8.2 Pre-annealed, post-annealed and 1-D hierarchical TiO_2 fibers displayed through SEM. *Source* Fig 8.2 is reproduced from author PhD thesis. Reference is https://shodhganga.inflibnet.ac.in/bitstream/10603/40981/15/15_synopsis.pdf

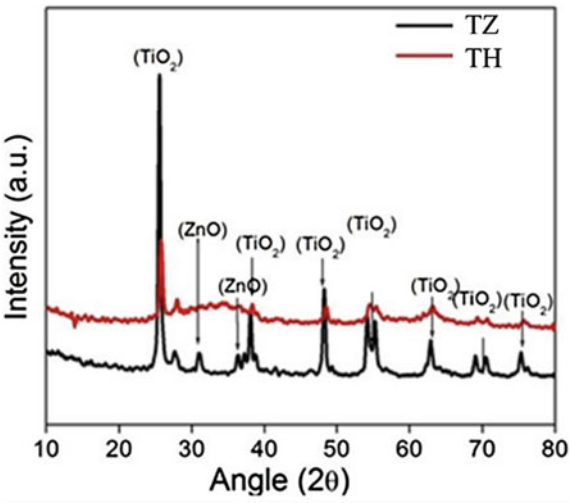

Fig. 8.3 XRD analysis of TZ and TH samples. *Source* Fig 8.3 is reproduced from author PhD thesis. Reference is https://shodhganga.inflibnet.ac.in/bitstream/10603/40981/15/15_synopsis.pdf

fiber. But it was observed that overall nanofiber morphology was maintained even after the etching process. Since the sublimation temperature of PVP is ~350 °C, no charring of the fibers occurred during the annealing at 450 °C.

Figure 8.3 shows the XRD pattern of the TZ fiber and TiO_2 hierarchical fiber. Distinct peaks of ZnO (wurtzite phase) and TiO_2 (anatase phase) could be seen in the spectrum (the TiO_2 and ZnO peaks are indexed in the XRD). No peaks of ZnO were observed in the hierarchical fiber which can be attributed to the complete removal of ZnO during the etching process. The surface area was calculated by the nitrogen adsorption–desorption experiments. The BET surface area of TZ fibers and TH fibers is ~53 and 78 m^2/g, respectively. This growth in surface area can be accredited to the selective etching of ZnO from the composite. Thus, through this simple approach, the surface area of TiO_2 could be enhanced by ~25%.

8.3.2 Photovoltaic Studies

The photocurrent (I_{sc}) and open-circuit voltage (V_{oc}) were measured using a Keithley 2400 digital source meter. The measurements were carried out under external applied potential for an exposed area of 0.2 cm^2. Figure 8.3 shows a typical photocurrent density–voltage (*J-V*) curves for TZF and TH fiber-based cells. The average performance characteristics obtained from the DSSC measurements are summarized in Table 8.1 and Fig. 8.4.

Current density of the cell depends on mainly dye loading and the efficiency of collecting the injected electrons from the metal oxide to the conducting glass substrate. From the above table, it can be observed that the performance of this TiO_2–ZnO system (TZ) was comparatively poor as compared to TiO_2 (TH) system. This

Table 8.1 Current, voltage and efficiency characteristics of DSSCs of TZ and TH samples

Samples	V_{oc} (V)	Jsc (mA/cm^2)	FF (%)	η (%)
TZ	0.78	11.05	67.5	5.99
TH	0.79	12.04	71.4	6.81

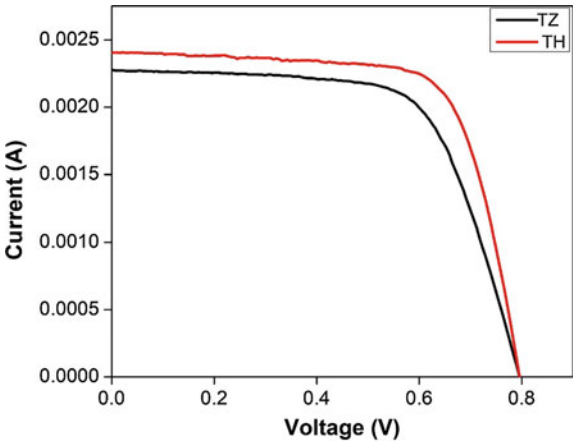

Fig. 8.4 Current–voltage (I–V) characteristics of DSSC using TZ and TH samples

can be attributed to the dye degradation by the formation of Zn^{+2}/dye complexes [24, 25]. This limits the charge carrier injection to the metal oxide and reduces the performance of the cells. As per the process explained in the above section, the bicomponent system is converted to the hierarchical structure by the selecting etching of one component, i.e., ZnO. Current density increases with an increase in porosity of the film, higher diffusion coefficient and higher concentration I_3^-. Recombination reactions are negative reactions which reduce the efficiency of the cell. These reactions are mainly occurring during the transport of electrons through the mesoporous TiO_2 layer. The increase in the current density of TH system could be attributed to the increased adsorption of dye due to the higher surface area. This was confirmed by the BET surface area. High surface area resulted in the binding of more dye molecules and hence better charge injection leading to high current density.

8.4 Conclusion

One-dimensional hierarchical shaped TZ fibers were fabricated from TiO_2–ZnO composite by electrospinning followed by selective etching of ZnO using dilute acetic acid. As synthesized anisotropic TiO_2 morphology by the above mentioned method exhibited high surface areas as compared to the TiO_2–ZnO composite. Morphological and phase analysis conducted by SEM and XRD studies conducted confirmed the anatase and hierarchical structure of one-dimensional morphology. Employing these

samples as photoanodes in DSSCs, a significant improvement in current density values was observed resulting in an efficiency of 6.8% for composites as compared with TZ with 6%.

Acknowledgements The author is grateful to Dr. Shanti Nair, Dean and Management of Amrita Center for Nano sciences, Kochi, for providing infrastructure and characterization facilities for conducting the research. Author would also like to thank Dr. A Sreekumaran Nair, MRF Limited, Chennai, for his guidance and other support for conducting the research.

References

1. R. Jose, V. Thavasi, S. Ramakrishna, Metal oxides for dye-sensitized solar cells. J. Am. Ceram. Soc. **92**, 289 (2009)
2. L. Schmidt-Mende, S.M. Zakeeruddin, M. Grätzel, Efficiency improvement in solid state-dye-sensitized photovoltaics with an amphiliphilic Ruthenium -dye. Appl. Phys. Lett. **86**, 013504 (2005)
3. M.L. Schmidt, U. Bach, B.R. Humphry, T. Horiuchi, H. Miura, S. Ito, S. Uchida, M. Grätzel, Organic dye for highly efficient solid state DSSC. Adv. Mater. **17**, 813 (2005)
4. S. Kim, J.K. Lee, S.O. Kang, J. Ko, J.-H. Yum, S. Fantacci, F. De Angelis, D. Di Censo, M.K. Nazeeruddin, M. Grätzel, Molecular engineering of organic sensitizers for solar cell applications. J. Am. Chem. Soc. **128**, 16701 (2006)
5. M. Zukalová, A. Zukal, L. Kavan, M.K. Nazeeruddin, P. Liska, M. Grätzel, Organized mesoporous TiO_2 films exhibiting greatly enhanced performance in dye-sensitized solar cells. Nano Lett. **5**(9), 1789 (2005). https://doi.org/10.1021/nl0514011
6. H. Yu, S. Zhang, H. Zhao, G. Will, P. Liu, An efficient and low-cost TiO_2 compact layer for performance improvement of dye-sensitized solar cells. Electrochim. Acta **54**(4), 1319 (2009)
7. R.Y. Ogura, S. Nakane, M. Morooka, M. Orihashi, Y. Suzuki, K. Noda, High-performance dye-sensitized solar cell with a multiple dye system Appl. Phys. Lett. **94**, 073308 (2009)
8. L. Hu, S. Dai, J. Weng, S. Xiao, Y. Sui, Y. Huang, S. Chen, F. Kong, X. Pan, L. Liang, K. Wang, Microstructure design of Nanoporous TiO_2 Photoelectrodes for Dye-Sensitized solar cell modules. J. Phys. Chem. B **111**, 358 (2007)
9. T. Berger, T. Lana-Villarreal, D. Monllor-Satoca, R. Gomez, In situ infrared study of the adsorption and surface acid − base properties of the Anions of Dicarboxylic acids at Gold Single Crystal and thin-film electrodes. J. Phys. Chem. C **111**, 9936 (2007)
10. D.D. Vuong, D.T.N. Tram, P.Q. Pho, N.D. Chienin, Phys. Eng. New Mater. 95–102
11. Z. Miao, D. Xu, J. Ouyang, G. Guo, X. Zhao, Y. Tang, Electrochemically induced Sol − Gel preparation of single-crystalline TiO_2 nanowires. Nano Lett. **2**, 717 (2002)
12. J.J. Wu, C.J. Yu, J. Phys. Chem. B **108**, 3377 (2004)
13. Y.W. Jun, M.F. Casula, J.H. Sim, S.Y. Kim, J. Cheon, A.P. Alivisatos, Surfactant-assisted elimination of a high energy facet as a means of controlling the shapes of TiO_2 nanocrystals. J. Am. Chem. Soc. **125**, 15981 (2003)
14. D. Li, Y. Xia, One-dimensional nanostructures: synthesis, characterization, and applications. Nano Lett. **3**, 555 (2003)
15. J.B. Baxter, E.S. Aydil, Dye-sensitized solar cells based on semiconductor morphologies with ZnO nanowires Sol. Energy Mater. Sol. Cells **90**, 607 (2006)
16. V.V. Kislyuk, O.P. Dimitriev, Nanorods and nanotubes for solar cells. J. Nanosci. Nanotechnol. **8**, 131 (2008)
17. A. Kumar, R. Jose, K. Fujihara, J. Wang, S. Ramakrishna, Structural and optical properties of electrospun TiO_2 nanofibers. Chem. Mater. **19**, 6536 (2007)

18. A. Hagfeldt, G. Boschloo, L. Sun, L. Kloo, H. Pettersson, Chem. Rev. **110**, 6595 (2010)
19. G.S. Anjusree, A. Sreekumaran Nair, S.V. Nair, S. Vadukumpully, One-pot hydrothermal synthesis of TiO_2/graphene nanocomposites for enhanced visible photocatalysis and photovoltaics. RSC Adv. (2013)
20. K. Sujith, A.M. Asha, P. Anjali, N. Sivakumar, K.R.V. Subramanian, S.V. Nair, A. Balakrishnan, Fabrication of highly porous conducting PANI-C composite fiber mats via electrospinning. Mater. Lett. **67**, 376 (2012)
21. A.A. Madhavan, A. Mohandas, A. Licciulli, K.P. Sanosh, P. Praveen, R. Jayakumar, S.V. Nair, A.S. Nair, A. Balakrishnan, Electrospun continuous nanofibers based on a TiO_2–ZnO-graphene composite, RSC Adv. **3**, 25312 (2013)
22. M. Asha, K. Sujith, P. Anjali, N. Sivakumar, K.R.V. Subramanian, S.V. Nair, A. Balakrishnan, Effect of surface nanomorphology and interfacial galvanic coupling of PEDOT-Titanium counter electrodes on the stability of dye-sensitized solar cell. J. Nanosci. Nanotechnol. **12**, 1 (2012)
23. M. Chen, H. Qu, J. Zhu, Z. Luo, A. Khasanov, A.S. Kucknoor, N. Haldolaarachchige, D.P. Young, S. Wei, Z. Guo, Polymer, **53**, 4501 (2012)
24. S.Y. Huang, G. Schlichthorl, A.J. Nozik, M. Grätzel, A.J. Frank, Charge recombination in dye-sensitized nanocrystalline TiO_2 solar cells, J. Phys. Chem. B, **101**, 2576 (1997)
25. H.B. Choi, S.O.J.J. Ko, G.H. Gao, H.S. Kang, M.S. Kang, M.K. Nazeeruddin, M. Grätzel, Angew. Chem, **121**, 6052 (2009)